# Supplementary Information for

## An essential role for EROS in redox-dependent endothelial signal transduction

Markus Waldeck-Weiermair[1,2]*, Apabrita A. Das[1], Taylor A. Covington[1], Shambhu Yadav[1], Jonas Kaynert[1], Ruby Guo[1], Priyana Balendran[3], Venkata Revanth Thulabandu[1], Arvind K. Pandey[1], Fotios Spyropoulos[1,4], David C. Thomas[3]*, and Thomas Michel[1]*

[1]Cardiovascular Division, Brigham and Women's Hospital, Harvard Medical School, Boston, USA.
[2]Molecular Biology and Biochemistry, Gottfried Schatz Research Center, Medical University of Graz, Neue Stiftingtalstraße 6/6, 8010, Graz, Austria
[3]Cambridge Institute of Therapeutic Immunology & Infectious Disease, University of Cambridge, Puddicombe Way, Cambridge CB2 0AW, UK
[4]Department of Pediatric Newborn Medicine, Brigham and Women's Hospital, Harvard Medical School,75 Francis Street, Boston, MA 02115,USA.

**To whom correspondence may be addressed. Email:**
*Corresponding authors: T.M.: thomas_michel@hms.harvard.edu; D.C.T.: tdct2@cam.ac.uk; M.W.-W.: mwaldeck-weiermair@bwh.harvard.edu.

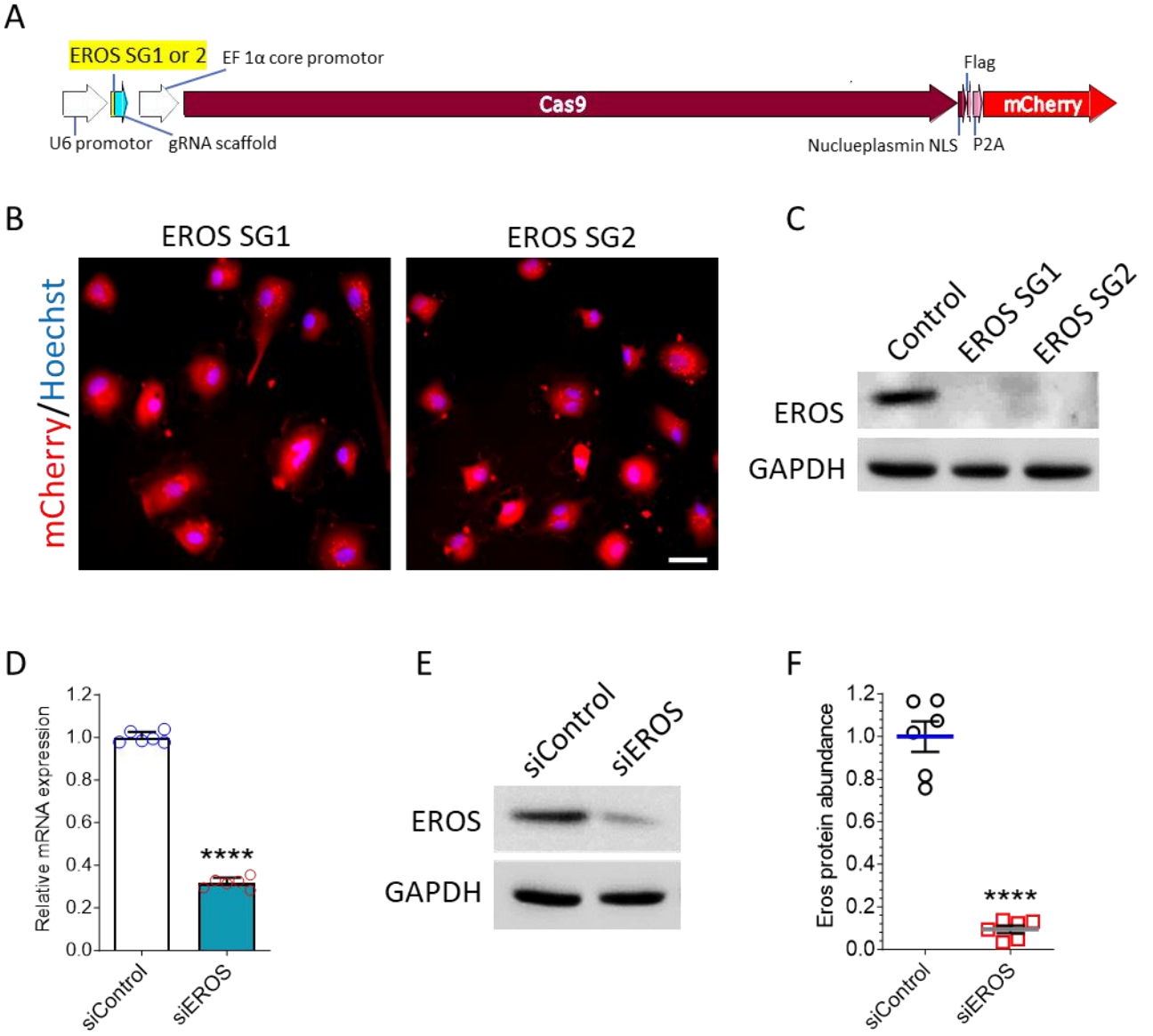


**Fig. S1: Validation of Eros knockout and knockdown endothelial model**

**A.** Topology of lentiviral CrispR/Cas9 construct highlighting position of Eros single-guide RNAs (yellow), Cas9 and fluorescent transduction marker mCherry (red). **B.** mCherry positive cells (red) indicate successful EROS SG 1 and 2 infection of HUVEC loaded with nuclear stain Hoechst (blue). Scale bar is 50 µm. **C.** EROS protein is undetectable in lysates from EROS SG transduced HUVEC versus CAS9 transduced cells (detailed analysis is provided in Fig. S4D). **D.** Bar graph presents relative EROS mRNA abundance in EROS knockdown endothelial cells. **E.** Immunoblot shows EROS protein abundance 3 days after siEROS transfection. **F.** Statistical analysis of siRNA-mediated EROS knockdown (red squares, n=6) versus siControl HUVEC (black circles, n=6). All values are presented as mean ± SEM, **** P<0.0001 using unpaired t test.

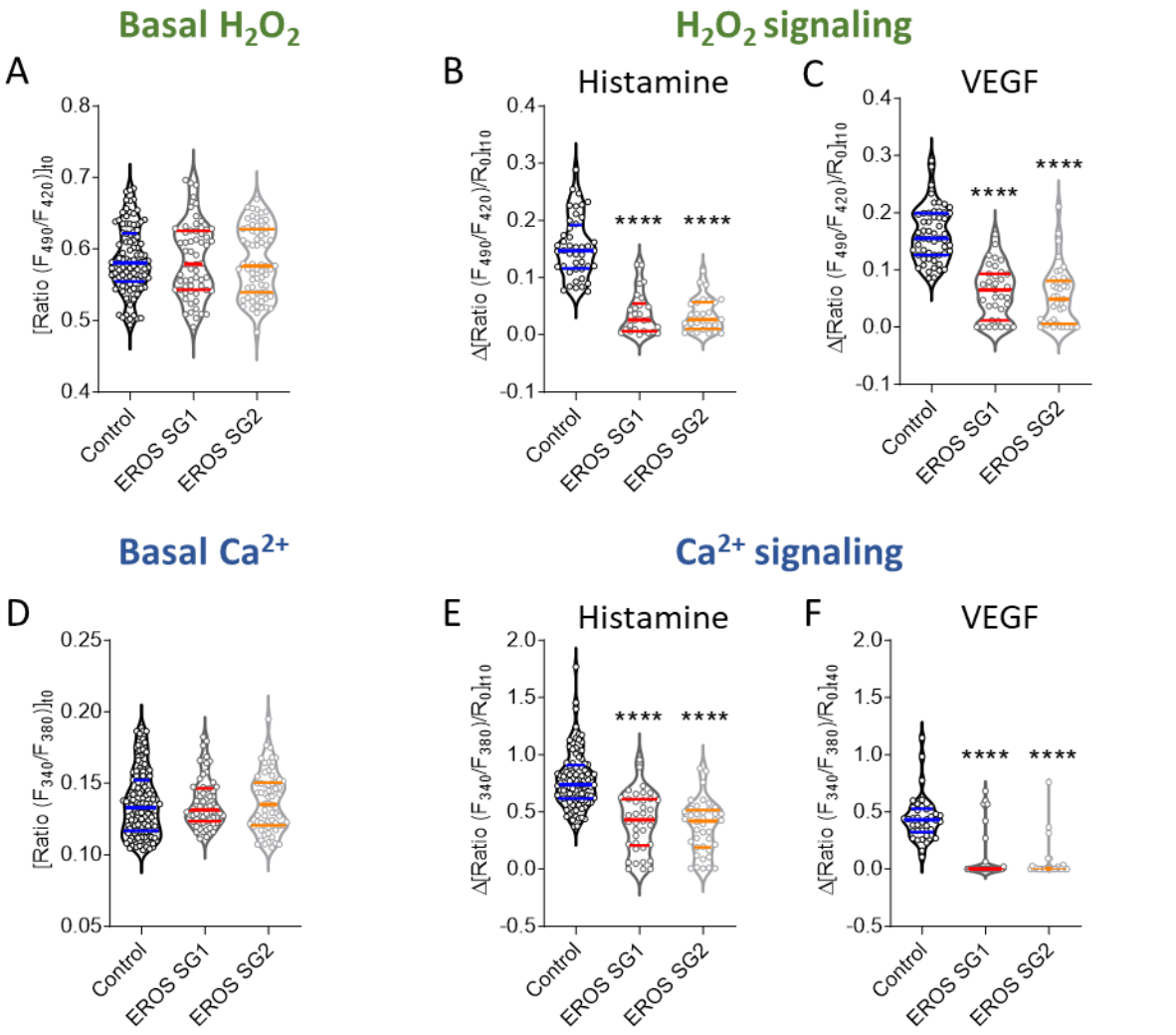


**Fig. S2: EROS knockout modulates agonist-induced $H_2O_2$ and $Ca^{2+}$ signaling**

**A.** Basal $H_2O_2$ levels of Hyper7 ratios do not differ between individual EROS knockout HUVEC for EROS SG1 (in dark gray, n=61), EROS SG2 (light gray, n=66) and Control (black, n=127) **B.** Analysis of HyPer7 responses to Histamine in individual EROS single guide RNA transduced HUVEC for EROS SG1 (dark gray, n=26), EROS SG2 (light gray, n=27) compared to Control cells (black, n=44) **C.** Detected maximum $H_2O_2$ levels of individual EROS SGs upon VEGF stimulation for Control (n=55), EROS SG1 (n=35) and EROS SG2 (n=39). **D.** No significant differences were found in basal $Ca^{2+}$ levels between individual EROS knockout cells for EROS SG1 (dark gray, n=64), EROS SG2 (light gray, n=66) and Control HUVEC (black, n=131) **E.** Statistical values of Fura2 measurements 10 minutes after histamine stimulation within individual EROS knockout cells showing single cell $Ca^{2+}$ levels in Cas9 infected HUVEC (Control, in black, n=93), in EROS SG1 mediated knockout (dark gray, n=38) or in EROS SG2 knockout HUVEC (light gray, n=40). **F.** Analysis of individual EROS SG $Ca^{2+}$ levels 40 minutes after VEGF treatment in EROS SG1 or SG2 HUVEC (n=26 each) versus Control (Control, n=38). Violin plots are marked with median and first and third quartiles for the graphed data, **** P<0.0001 using 1way ANOVA..

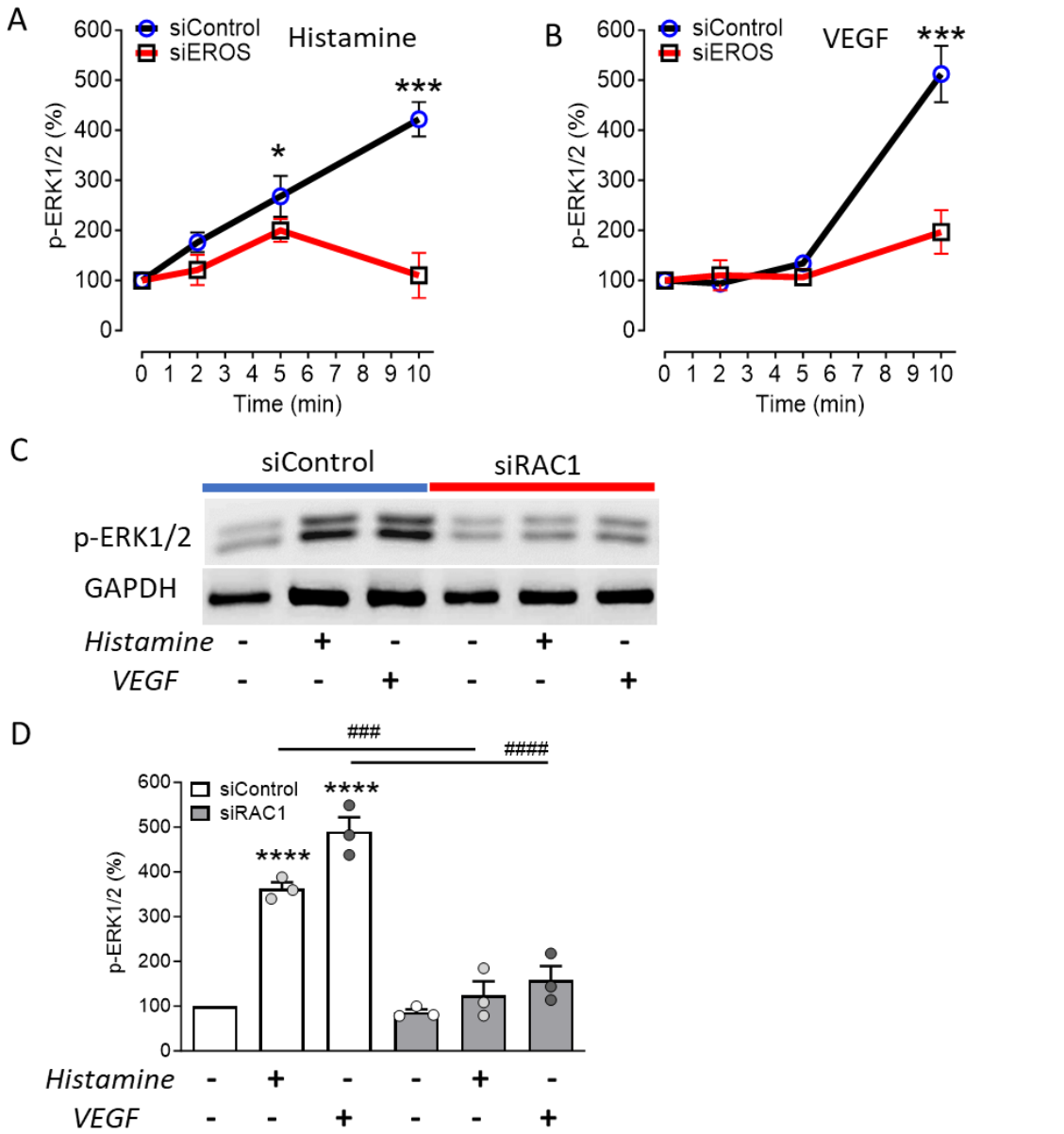


**Fig. S3: EROS and RAC1 knockdown similarly inhibit the time-dependent ERK1/2 phosphorylation in response to histamine and VEGF**

**A.** ERK1/2 phosphorylation of protein lysates after siRNA-mediated knockdown using EROS or control siRNA, analyzed at the times indicated after adding histamine (n=3 for each time point) or **B.** in response to VEGF. **C.** Representative immunoblot of ERK1/2 phosphorylation 10 minutes after histamine or VEGF stimulation after siRNA-mediated RAC1 knockdown (siRAC1) versus Control cells (siControl). **D.** Statistical evaluation of phosphorylated ERK1/2 normalized to GAPDH abundances. Both histamine and VEGF induce ERK1/2 phosphorylation that is blocked by RAC1 siRNA treatment (n=3 for each condition). All values are presented as mean ± SEM, * P<0.05, *** P<0.001 and **** P<0.0001 compared to untreated siControl HUVEC and ### P<0.001 or #### P<0.0001 compared to same stimulations, either histamine or VEGF following siRNA-mediated knockdown of RAC1 vs. control siRNA, analyzed using 1way ANOVA.

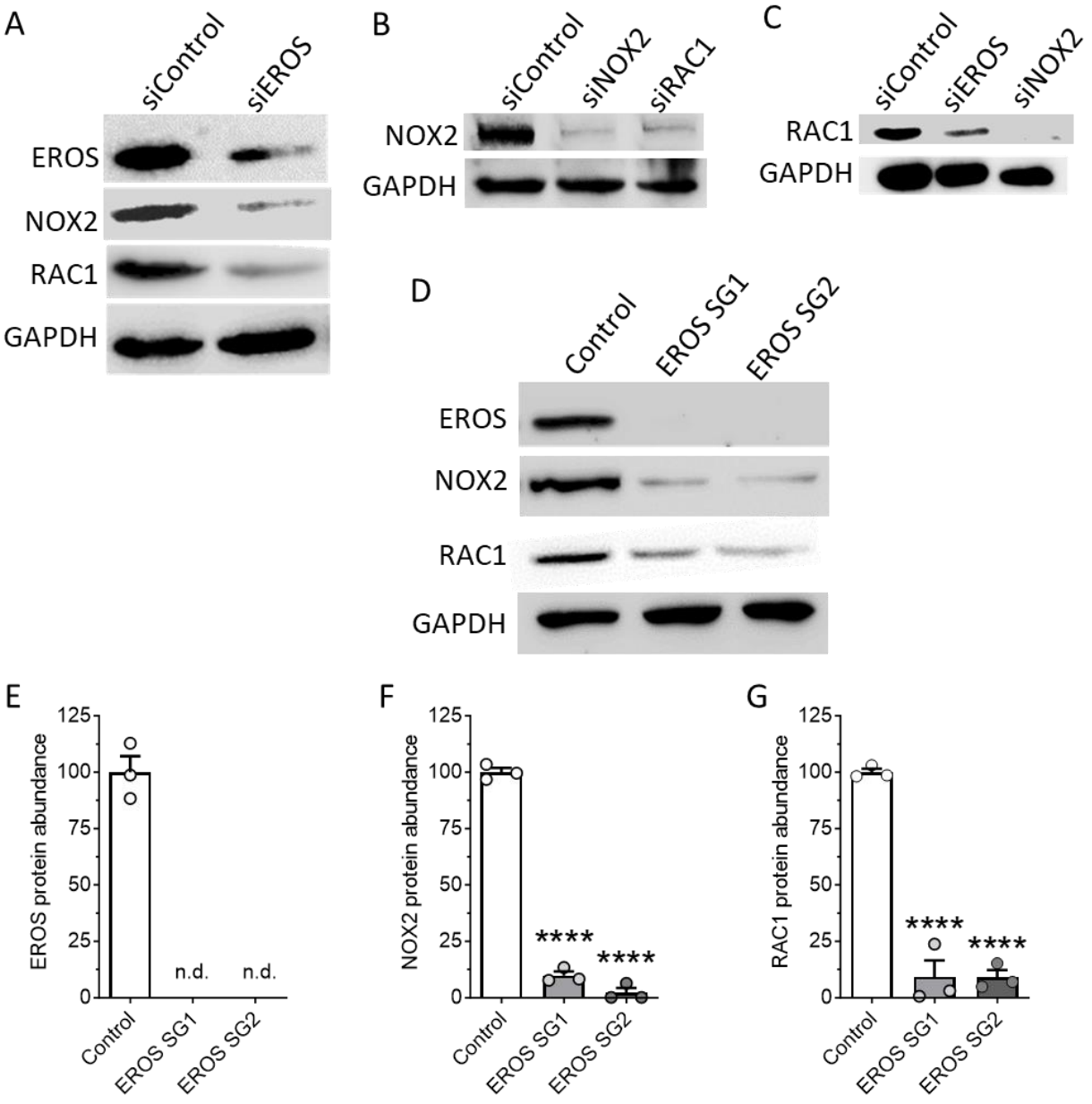


**Fig. S4: Interrelated regulation of EROS, NOX2 and RAC1 in knockdown and knockout HUVEC** **A.** This panel shows a representative immunoblot probed with antibodies as indicated following siRNA-mediated knockdown of EROS. **B.** Representative blot shows lower RAC1 abundance in siNOX2 compared to siEROS (statistic significance as shown in the legend to Fig. 2G). **C.** Immunoblot of HUVEC following siRNA-mediated knockdown of RAC1. **D.** Representative immunoblots of EROS knockout HUVEC (EROS SG1 or SG2) versus Control show lower abundances of RAC1 and NOX2. While EROS remained undetectable, **E.** Quantitation of EROS following CRISPR/Cas9-mediated EROS knockout in HUVEC (n=3). **F.** Relative NOX2 protein abundance in individual EROS (SG1 or SG2) knockout cells versus Control (n=3 each). **G.** Effect of EROS knockout on RAC1 abundance (n=3 each). **** P<0.0001 using 1way ANOVA.

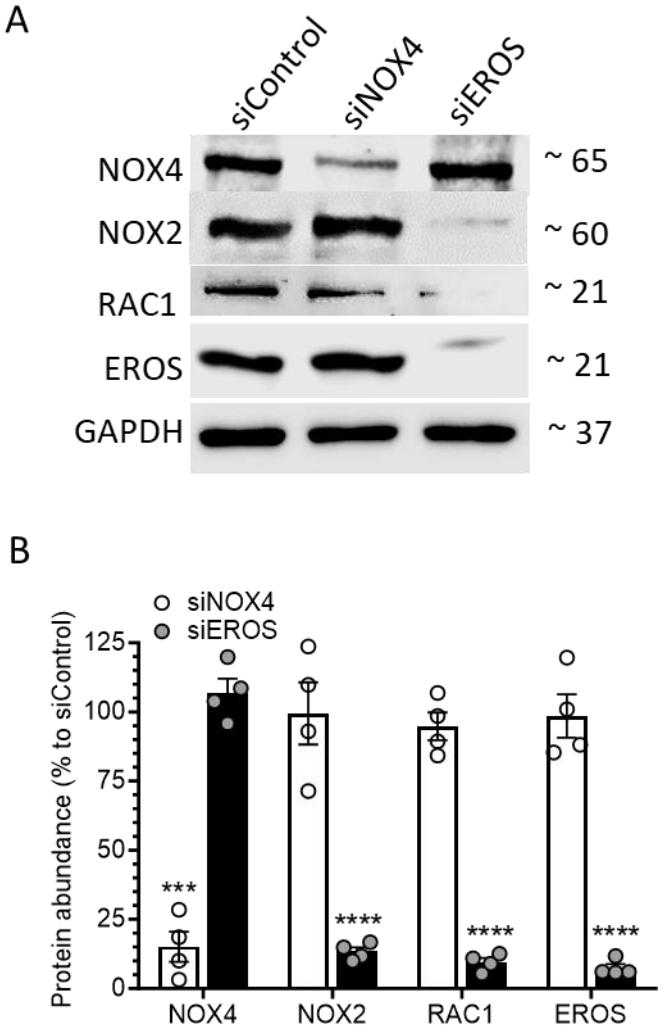


**Fig. S5: Effects of siRNA-mediated EROS knockdown on the abundance of NOX4, and vice versa**

**A.** Representative immunoblots probed with antibodies directed against NOX4, NOX2, RAC1 and EROS in HUVEC transfected with siRNA targeting NOX4 or EROS or control are shown. Molecular weights of observed bands are indicated in kDa. **B.** Statistical evaluation of 4 independent immunoblot experiments in HUVEC following siRNA mediated NOX4 knockdown (white bars), or following siRNA-mediated knockdown of NOX2, RAC1 and EROS as shown (gray bars). *** indicates $P<0.001$ and **** $P<0.0001$ (2-way ANOVA).

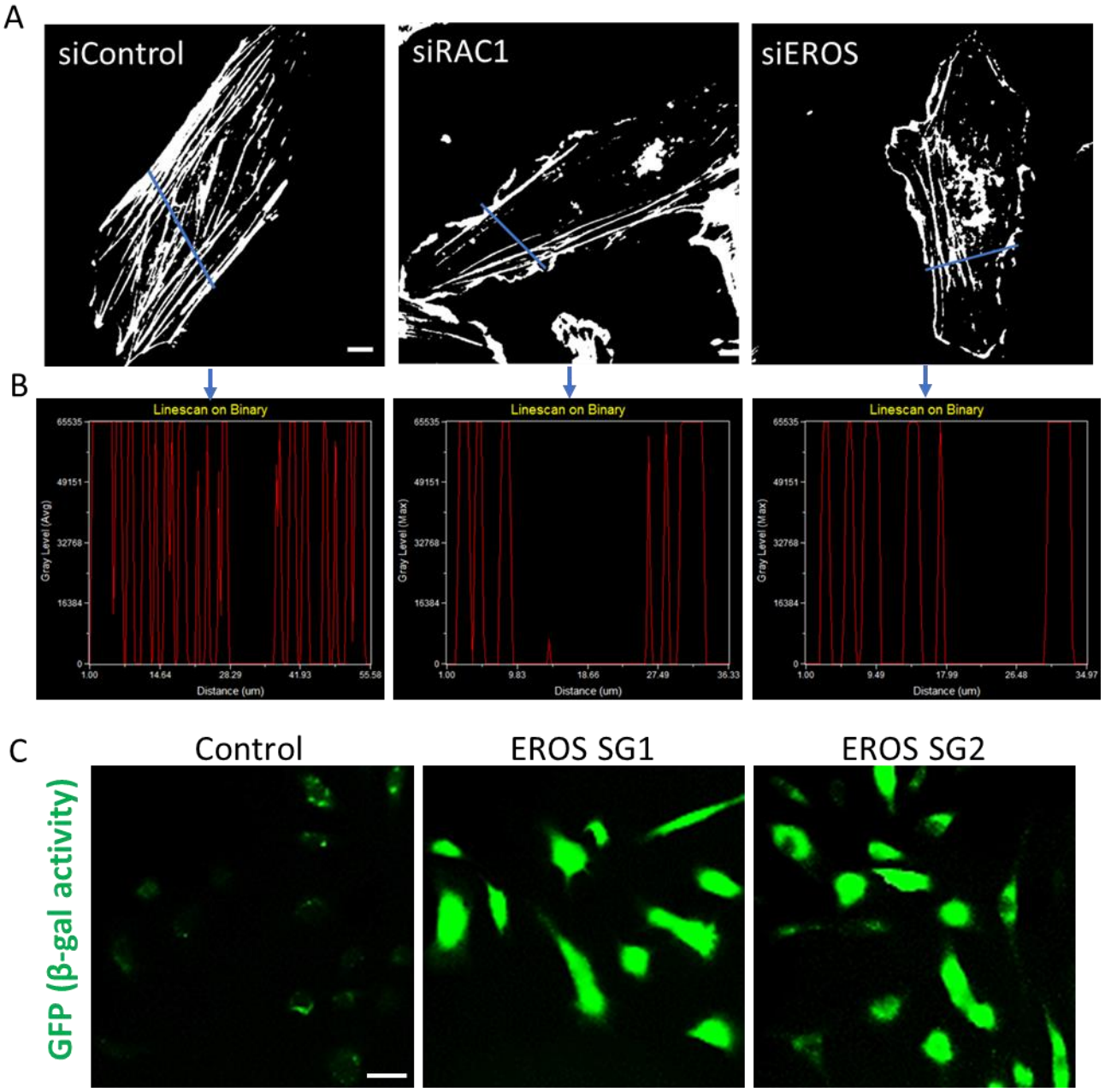


**Fig. S6: EROS and RAC1 knockdown HUVEC show disrupted cytoskeleton and EROS knockout shows marked signs of senescence**

**A.** Representative images from Fig. 3A-C of phalloidin-stained HUVEC transfected with siRNA targeting RAC1 or EROS were binarized and subjected to LineScan analysis by assessing a line through the region with highest actin filament abundance (blue line). Scale bar is 10 µm. **B.** Individual LineScans of the respective siRNA-treated cells show the number of filaments (red peaks). The abundance of intact actin filaments was then calculated relative to line length and expressed as filaments per 10 µm. **C.** Fluorescence microscopic images show intensities of ß-galactosidase activity as a marker for cellular senescence in EROS knockout HUVEC (EROS SG1 and EROS SG2) vs. control cells (Control). Scale bar is 50 µm.

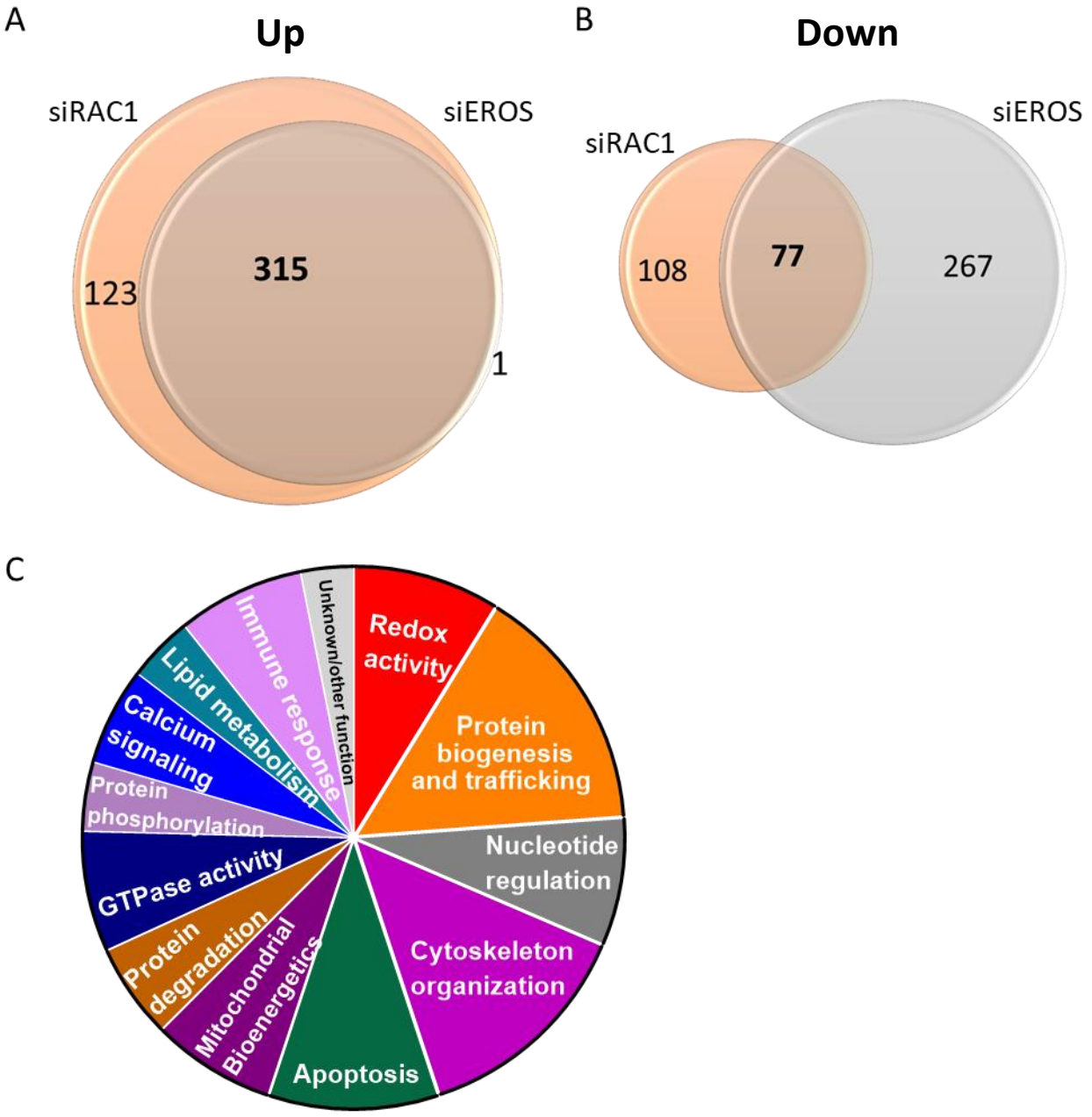


**Fig. S7: Overlap of shared up- or downregulated proteins of RAC1 and EROS knockdown**
**A.** Venn diagram show that almost all upregulated proteins (> 2-fold) in siEROS treated HUVEC were also upregulated after knockdown of RAC1. **B.** Proteomic analyses detected more downregulated proteins (< 0.5-fold) in samples of EROS knockdown, a significant overlap with those in siRAC1 samples were detectable. Numbers of shared proteins are shown in bold and regular numbers indicate unique regulated proteins. **C.** Pie chart presents Gene Ontology analysis of shared protein regulation within EROS or RAC1 siRNA-mediated downregulation sorted according to various categories of their biological function (Data S3 lists sorted proteins).

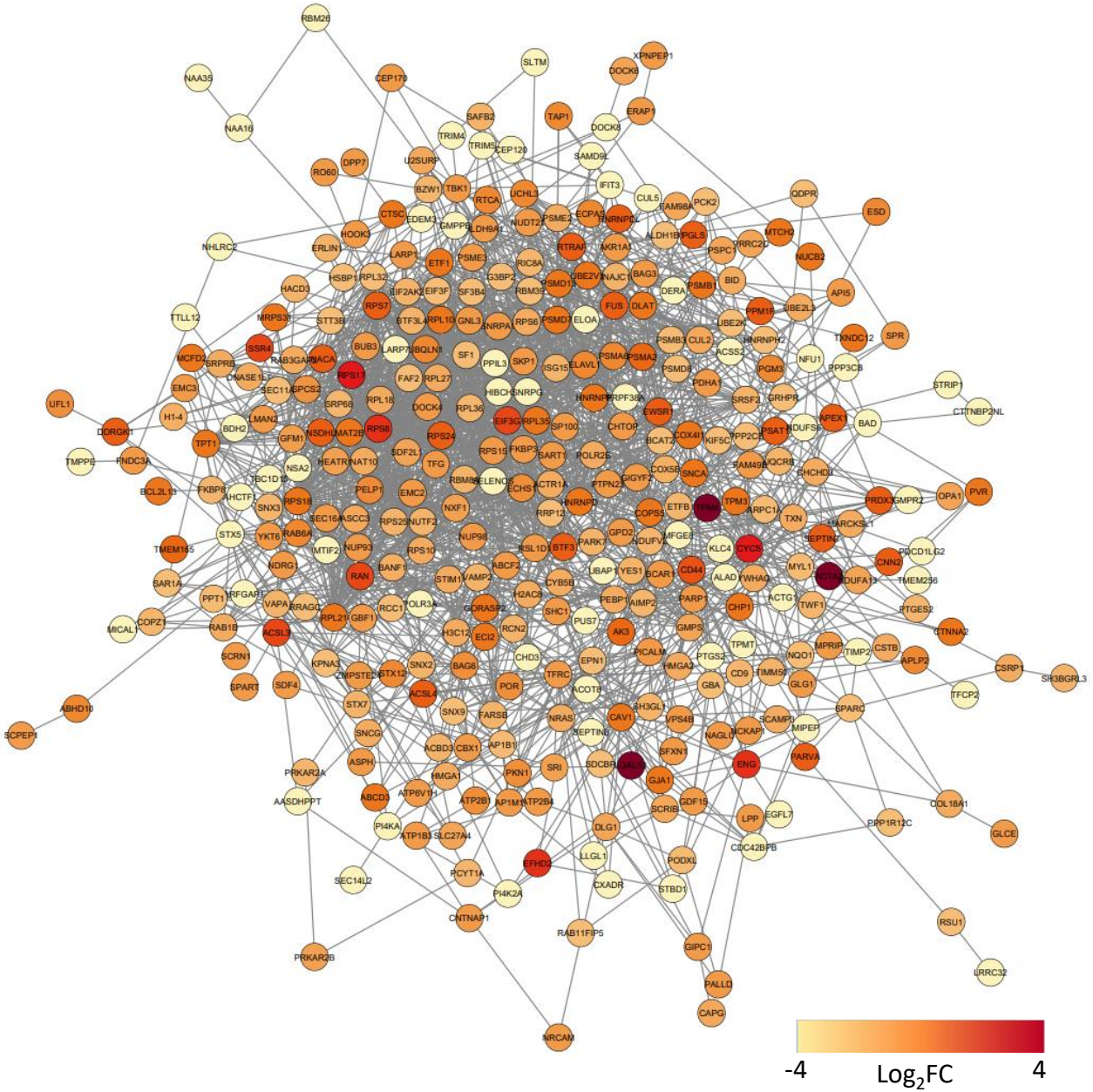


**Fig. S8: Full network analysis for common protein regulations upon EROS and RAC1 knockdown**

| Primer Name | Sequence (5’-3’) | cds Position / PAM sequence | Accession Number |
|---|---|---|---|
| EROS SG1 sense | *CACC*GCCATCTTCGACAAGAGCAC | 205 / AGG | NM_001100407.3 |
| EROS SG1 antisense | *AAAC*GTGCTCTTGTCGAAGATGGC | 225 | NM_001100407.3 |
| EROS SG2 sense | *CACC*GGTGGTGCTCCGGCTTGCGA | 374 / CGG | NM_001100407.3 |
| EROS SG2 antisense | *AAAC*TCGCAAGCCGGAGCACCACC | 394 | NM_001100407.3 |
| | | **mRNA Position** | |
| EROS RT for | CCCAGTGGTACTTTGGTGCC | 141 | NM_001100407.3 |
| EROS RT rev | GCGGTCATGTACTTCTGTCCC | 264 | NM_001100407.3 |
| NOX2 RT for | TGGAGAGCCAGATGCAGGAA | 1401 | NM_000397.4 |
| NOX2 RT rev | TCCTCATCATGGTGCACAGC | 1512 | NM_000397.4 |
| NOX4 RT for | CTGTGGTGTTACTATCTGTATTTTCTC | 450 | NM_016931.5 |
| NOX4 RT rev | CTTGCTGCATTCAGTTCAACA | 563. | NM_016931.5 |
| RAC1 RT for | GGCTAAGGAGATTGGTGCTG | 644 | NM_006908.5 |
| RAC1 RT rev | AGAGGACTGCTCGGATCGCT | 741 | NM_006908.5 |
| RPOL2 RT for | TCCAGAGCGAGTGCATGAGA | 1050 | NM_000937.5 |
| RPOL2 RT rev | CAATCATCCACTCTGGCCGT | 1147 | NM_000937.5 |
| **siRNA Name** | **Sense sequence (5’-3’)** | **mRNA Position** | **Accession Number** |
| siControl | UUCUCCGAACGUGUCACGUdTdT | (scrambled) | - |
| siEROS_1 | AAGCUCAUCACCAGCUUCCUGdTdT | 606 | NM_001100407.3 |
| siEROS_2 | AAGGUCAGCUCUUCUAGUAdTdT | 1451 | NM_001100407.3 |
| siNOX2_1 | ACCAAGGAGUAGCUAUAUAdTdT | 2173 | NM_000397.4 |
| siNOX2_2 | AGAGAAUAAAGAACCCUGAdTdT | 4276 | NM_000397.4 |
| siNOX4_1 | ACAGUGAAGACUUUGUUGAACUGAAdTdT | 530 | NM_016931.5 |
| siNOX4_2 | AUCUGGUGGAGGUAGUGAUACUCUGdTdT | 275 | NM_016931.5 |
| siRAC1_1 | UGCAUUUCCUGGAGAAUAUdTdT | 287 | NM_006908.5 |
| siRAC1_2 | CACUCCCAUCAUCCUAGUGdTdT | 530 | NM_006908.5 |

**Table S1:** The list shows the primer sequences used in EROS SG RNA cloning and qRT-PCR procedures and gene-specific siRNA sense strand sequences.

| Gene | Full Name | R/C | E/C | Description / Reductive stress response (RSR) | Ref. |
|---|---|---|---|---|---|
| **AASDHPPT** | L-aminoadipate-semialdehyde dehydrogenase-phosphopantetheinyl transferase | 0.5 | 0.2 | Associated with TPMT<br>RSR modulated | (1) |
| **ACSL3** | Fatty acid CoA ligase ACSL3 | 6 | 6 | Modulate fatty acid β-oxidation in quiescent endothelial cells | (2) |
| **ACSL4** | Long-chain-fatty-acid-CoA ligase 4 | 5 | 5 | | (2) |
| **BUB3** | Mitotic checkpoint protein BUB3 | 3 | 2.5 | Cell cycle arrest marker; required for DTT resistance | (3) |
| **CAV1** | Caveolin-1 | 4 | 4 | Negatively regulates eNOS activity | (4) |
| **COX5B** | Cytochrome c oxidase subunit 5B | 2.5 | 2 | In Complex IV, Upreg. in hypoxia | (5) |
| **CUL2** | Cullin-2 | 2.6 | 2 | Recruited scaffold in RSR | (6) |
| **CUL5** | Cullin-5 | 0.5 | 0.2 | Regulates endothelial growth | (7) |
| **CYB5B** | Cytochrome b5 type B | 2.5 | 2 | Regulates eNOS activity | (8) |
| **CYCS** | Cytochrome c | 8 | 9 | Pro-apoptotic | (9) |
| **CYRIB** | CYFIP-related RAC1 interactor B | 3 | 2.8 | Bind RAC1, suppress protrusions | (10) |
| **ENG** | Endoglin | 7 | 7 | Upregulated in hypoxia;<br>Modulates eNOS activity | (11, 12)<br>(13) |
| **GMPR2** | GMP reductase 2 | 0.5 | 0.3 | Converts GMP to IMP | (14) |
| **MARCKSL1** | MARCKS-related protein | 2.5 | 2 | Retard migration | (15) |
| **MICAL1** | [F-actin]-monooxygenase MICAL1 | 0.5 | 0.3 | F-actin dismantling oxidase | (16) |
| **NDUFS6** | NADH dehydrogenase iron-sulfur protein 6 mitochondrial | 0.5 | 0.2 | Complex I subunit, downregulation leads to senescence | (17) |
| **NFU1** | NFU1 iron-sulfur cluster scaffold homolog mitochondrial | 0.5 | 0.3 | Scaffold for iron-sulfur cluster<br>Downregulated in hypoxia | (18) |
| **NQO1** | NAD(P)H dehydrogenase [quinone] 1 | 2 | 2 | Upregulated in RSR induced by various antioxidant treatments | (19–21) |
| **OPA1** | Dynamin-like 120 kDa protein mitochondrial | 2.7 | 2 | Upregulated by carnosic acid (antioxidant from rosemary) | (22) |
| **PARK7** | Parkinson disease protein 7 | 2.3 | 2 | Upregulated in response to Vit. E | (23) |
| **PRDX3** | Thioredoxin-dependent peroxide reductase mitochondrial | 5 | 4.4 | Upregulated in RSR induced by various antioxidant treatments | (24–27) |
| **QDPR (DHPR)** | Dihydropteridine reductase | 2 | 2 | Catalyzes reduction of quinones via NADH (BH2 to BH4); Upregulateed by the antioxidant sophoridine | (28) (29) |
| **SACM1L** | Phosphatidylinositol-3-phosphatase SAC1 | 3 | 2.5 | Associated with ER stress | (30) |
| **SELENOS** | Selenoprotein S | 0.5 | 0.2 | Antioxidant, Downregulation reduces SOD activity and upregulates CAV1 in HUVEC | (31) |
| **SNCA** | Alpha-synuclein | 4 | 4 | Reduces mitochondrial inactivity via Nrf2 | (32) |
| **TFRC** | Transferrin receptor protein 1 | 3 | 2.6 | Upregulated in hypoxia | (33) |
| **TPMT** | Thiopurine S-methyltransferase | 0.5 | 0.1 | RSR modulated | (1) |
| **TRIO** | Triple functional domain protein | 3 | 3 | Main GEF for RAC1 in HUVEC | (34) |
| **TXN** | Thioredoxin | 2.5 | 2 | Upregulated in RSR induced by various antioxidant treatments | (23, 35) |
| **TXNDC12** | Thioredoxin domain-containing protein 12 | 4 | 4 | Upregulated in ER stress | (36, 37) |

**Table S2: GO annotated key proteins regulated upon EROS and RAC1 knockdown**
R/C: Fold change in protein abundance of siRAC1 : siControl, E/C: Fold change siEROS : siControl

**Data S1-S5:** Excel spreadsheets list detailed results of various proteomic analyses used for compilation of Fig. 4, 5A, B, Fig. S7, S8 and Table S2.

**SI References:**


1. A. Šmid, *et al.*, Transcriptome analysis reveals involvement of thiopurine S-methyltransferase in oxidation-reduction processes. *European Journal of Pharmaceutical Sciences* **192** (2024).

2. J. Kalucka, *et al.*, Quiescent Endothelial Cells Upregulate Fatty Acid β-Oxidation for Vasculoprotection via Redox Homeostasis. *Cell Metabolism* **28**, 881-894.e13 (2018).

3. J. D. Rand, C. M. Grant, The thioredoxin system protects ribosomes against stress-induced aggregation. *Molecular Biology of the Cell* **17** (2006).

4. Z. Chen, *et al.*, Nitric oxide-dependent Src activation and resultant caveolin-1 phosphorylation promote eNOS/caveolin-1 binding and eNOS inhibition. *Molecular Biology of the Cell* **23**, 1388–1398 (2012).

5. P. R. Castello, *et al.*, Oxygen-regulated isoforms of cytochrome c oxidase have differential effects on its nitric oxide production and on hypoxic signaling. *Proceedings of the National Academy of Sciences of the United States of America* **105**, 8203–8208 (2008).

6. A. G. Manford, *et al.*, A Cellular Mechanism to Detect and Alleviate Reductive Stress. *Cell* **183**, 46-61.e21 (2020).

7. A. Buchwalter, *et al.*, Expression of VACM-1/cul5 mutant in endothelial cells induces MAPK phosphorylation and maspin degradation and converts cells to the angiogenic phenotype. *Microvascular Research* **75**, 155–168 (2008).

8. C. E. Sparacino-Watkins, *et al.*, Nitrite reductase and nitric-oxide synthase activity of the mitochondrial molybdopterin enzymes mARC1 and mARC2. *Journal of Biological Chemistry* **289**, 10345–10358 (2014).

9. D. Chandra, J. W. Liu, D. G. Tang, Early mitochondrial activation and cytochrome c up-regulation during apoptosis. *Journal of Biological Chemistry* **277**, 50842–50854 (2002).

10. L. Fort, *et al.*, Fam49/CYRI interacts with Rac1 and locally suppresses protrusions. *Nature Cell Biology* **20**, 1159–1171 (2018).

11. Y. Yang, Y. Song, J. Loscalzo, Regulation of the protein disulfide proteome by mitochondria in mammalian cells. *Proceedings of the National Academy of Sciences of the United States of America* **104**, 10813–10817 (2007).

12. T. Sánchez-Elsner, L. M. Botella, B. Velasco, C. Langa, C. Bernabéu, Endoglin expression is regulated by transcriptional cooperation between the hypoxia and transforming growth factor-β pathways. *Journal of Biological Chemistry* **277**, 43799–43808 (2002).

13. Y.-S. Jang, I.-H. Choi, Contrasting Roles of Different Endoglin Forms in Atherosclerosis. *Immune Network* **14**, 237 (2014).

14. S. Saveljeva, *et al.*, A purine metabolic checkpoint that prevents autoimmunity and autoinflammation. *Cell Metabolism* **34**, 106-124.e10 (2022).

## SI References (continued):


15. B. Björkblom, *et al.*, c-Jun N-Terminal Kinase Phosphorylation of MARCKSL1 Determines Actin Stability and Migration in Neurons and in Cancer Cells. *Molecular and Cellular Biology* **32**, 3513–3526 (2012).

16. H. Wu, H. G. Yesilyurt, J. Yoon, J. R. Terman, The MICALs are a Family of F-actin Dismantling Oxidoreductases Conserved from Drosophila to Humans. *Scientific Reports* **8** (2018).

17. Y. Zhang, *et al.*, Adult mesenchymal stem cell ageing interplays with depressed mitochondrial Ndufs6. *Cell Death and Disease* **11** (2020).

18. A. Melber, *et al.*, Role of Nfu1 and Bol3 in iron-sulfur cluster transfer to mitochondrial clients. *eLife* **5**, 1–24 (2016).

19. S. Sunny, *et al.*, Tandem Mass Tagging Based Identification of Proteome Signatures for Reductive Stress Cardiomyopathy. *Frontiers in Cardiovascular Medicine* **9** (2022).

20. G. Shanmugam, *et al.*, Reductive Stress Causes Pathological Cardiac Remodeling and Diastolic Dysfunction. *Antioxidants and Redox Signaling* **32**, 1293–1312 (2020).

21. R. Wufuer, *et al.*, Distinct Roles of Nrf1 and Nrf2 in Monitoring the Reductive Stress Response to Dithiothreitol (DTT). *Antioxidants* **11** (2022).

22. C. Y. Lin, W. J. Chen, R. H. Fu, C. W. Tsai, Upregulation of OPA1 by carnosic acid is mediated through induction of IKKγ ubiquitination by parkin and protects against neurotoxicity. *Food and Chemical Toxicology* **136** (2020).

23. R. S. Duncan, A. Keightley, A. A. Lopez, C. W. Hall, P. Koulen, Proteome changes in a human retinal pigment epithelial cell line during oxidative stress and following antioxidant treatment. *Frontiers in Immunology* **14**, 1–14 (2023).

24. E. Peris, *et al.*, Antioxidant treatment induces reductive stress associated with mitochondrial dysfunction in adipocytes. *Journal of Biological Chemistry* **294**, 2340–2352 (2019).

25. N. Miyamoto, *et al.*, Quercetin induces the expression of peroxiredoxins 3 and 5 via the Nrf2/NRF1 transcription pathway. *Investigative Ophthalmology and Visual Science* **52**, 1055–1063 (2011).

26. S. Poncin, I. M. Colin, A. C. Gérard, Minimal oxidative load: A prerequisite for thyroid cell function. *Journal of Endocrinology* **201**, 161–167 (2009).

27. A. B. Sikiru, *et al.*, Elucidation of the liver proteome in response to an antioxidant intake in rabbits. *Egyptian Liver Journal* **11** (2021).

28. J. Vasquez-Vivar, Z. Shi, S. Tan, Tetrahydrobiopterin in Cell Function and Death Mechanisms. *Antioxidants and Redox Signaling* **37**, 171–183 (2022).

29. Y. Chen, *et al.*, Research progress of sophoridine's pharmacological activities and its molecular mechanism: an updated review. *Frontiers in Pharmacology* **14** (2023).

## SI References (continued):


30. W. Li, P. Liu, H. Liu, F. Zhang, Y. Fu, Integrative analysis of genes reveals endoplasmic reticulum stress-related immune responses involved in dilated cardiomyopathy with fibrosis (Apoptosis, (2023), 28, 9-10, (1406-1421), 10.1007/s10495-023-01871-z). *Apoptosis* **28**, 1422 (2023).

31. Y. Zhao, *et al.*, Effects of selenoprotein S on oxidative injury in human endothelial cells. *Journal of Translational Medicine* **11**, 1–8 (2013).

32. M. H. Fu, *et al.*, Nrf2 activation attenuates the early suppression of mitochondrial respiration due to the α-synuclein overexpression. *Biomedical Journal* **41**, 169–183 (2018).

33. Y. Pan, *et al.*, TFRC in cardiomyocytes promotes macrophage infiltration and activation during the process of heart failure through regulating Ccl2 expression mediated by hypoxia inducible factor-1α. *Immunity, Inflammation and Disease* **11** (2023).

34. A. Klems, *et al.*, The GEF Trio controls endothelial cell size and arterial remodeling downstream of Vegf signaling in both zebrafish and cell models. *Nature Communications* **11** (2020).

35. A. Carretero, *et al.*, Early reductive stress and late onset overexpression of antioxidant enzymes in experimental myocardial infarction. *Free Radical Research* **54**, 173–184 (2020).

36. L. Tang, *et al.*, TXNDC12 inhibits lipid peroxidation and ferroptosis. *iScience* **26**, 108393 (2023).

37. N. Swain, *et al.*, Aberrant Upregulation of Compensatory Redox Molecular Machines May Contribute to Sperm Dysfunction in Infertile Men with Unilateral Varicocele: A Proteomic Insight. *Antioxidants and Redox Signaling* **32**, 504–521 (2020).